



Performance of PDMS membranes in pervaporation: Effect of silicalite fillers and comparison with SBS membranes

A. Dobrak^{a,b}, A. Figoli^{c,*}, S. Chovau^a, F. Galiano^c, S. Simone^c, I.F.J. Vankelecom^b, E. Drioli^c, B. Van der Bruggen^{a,*}

^a Department of Chemical Engineering, Laboratory of Applied Physical Chemistry and Environmental Technology, Katholieke Universiteit Leuven, W. de Croylaan 46, B-3001 Leuven, Belgium

^b Department of Microbial and Molecular Systems, Centre for Surface Chemistry and Catalysis, Katholieke Universiteit Leuven, Kasteelpark Arenberg 23, B-3001 Leuven, Belgium

^c Research Institute on Membrane Technology (ITM-CNR), c/o University of Calabria, via P. Bucci, Cubo 17/C, 87030 Rende, Cosenza, Italy

ARTICLE INFO

Article history:

Received 5 October 2009

Accepted 11 February 2010

Available online 14 February 2010

Keywords:

PDMS membranes

Pervaporation

Solution-diffusion model

Temperature effect

Membrane performance

ABSTRACT

Laboratory-made silicalite filled PDMS membranes were tested by means of concentration and temperature influence on the membrane performance in removal of ethanol from ethanol/water mixtures. This allowed studying the applicability of solution-diffusion model in the transport mechanism description. Experiments were performed by varying the ethanol concentration in the feed and temperature. Two types of fillers were incorporated into the PDMS network: commercial zeolite silicalite (CBV 3002) and laboratory-made colloidal silicalite-1. Obtained results were then compared with data gathered for unfilled PDMS membranes to examine the effect of fillers incorporation. Moreover, the comparison with novel block co-polymer based porous and dense SBS membranes was done. It was found that the solution-diffusion model was a good representation of ethanol transport through both filled and unfilled PDMS membranes, whereas the water flux did not obey this model due to the swelling effects. Incorporation of the fillers increased membrane stability and improved the selectivity. Performance of the SBS membranes characterized by a dense structure was found to be similar to the performance of filled PDMS membranes.

© 2010 Elsevier Inc. All rights reserved.

1. Introduction

Pervaporation is a membrane separation technique in which a liquid mixture is partially vaporized during transport through a membrane by means of vacuum at the permeate side. This process is commonly classified into three different groups depending on the feed type and aim of the separation: hydrophilic, hydrophobic and target organophilic pervaporation [1]. Among them the most studied process is pervaporation with hydrophilic membranes, which involves either dehydration of organic compounds or water extraction from a mixture [2–4]. On the other hand, hydrophobic pervaporation could be of potential use in the industry, as an easy and economical method of either organic solvents recovery, removal of alcohol from alcoholic beverages, or recovery of aroma compounds from fruit juices [5–8]. Typical applications of organophilic pervaporation include separation of organic compounds mixtures, such as benzene/cyclohexane and methanol/methyl-tert-butyl ether (MTBE) [9,10].

* Corresponding authors. Fax: +39 984 40 2103 (A. Figoli), +32 16 322991 (B. Van der Bruggen).

E-mail addresses: A.Figoli@itm.cnr.it (A. Figoli), Bart.VanderBruggen@cit.kuleuven.be (B. Van der Bruggen).

Pervaporation was also found to be a good alternative to conventional processes, such as distillation or extraction, due to the simplicity of operation, low working cost and reduced amounts of chemicals required. Several applications in the separation of mixtures containing isomers, compounds with close boiling points, or mixtures containing azeotropes were already reported in the literature [11,12].

Because of increasing interest in this membrane technique, a lot of research is currently carried out in order to develop membranes suitable for specific applications. The most common polymer used in the membrane synthesis for hydrophobic pervaporation is polydimethylsiloxane (PDMS) [6]. This elastomer, containing a siloxane (Si–O) backbone substituted with methyl groups, is widely known also in gas separation and solvent resistant nanofiltration, because of its high chemical stability and highly hydrophobic character [13]. Additionally, inorganic membranes based on hydrophobic zeolites were tested by different authors and showed superior membrane performance characteristics [14–17]. Hence, the necessity of introducing fillers such as zeolites into the polymeric network seemed to be interesting and became the aim of scientific investigation [18,19]. It was already shown that nanofillers other than zeolites have a beneficial effect in other membrane processes such as pressure driven filtration [20] and gas separation [21]. The

effect of filler concentration in such membranes is subject to specific studies in which diverse effects have to be investigated, such as fouling resistance [22] separation and permeability [23] or gas solubility [21]. In the latter publication, a solution-diffusion model equation was used to describe fluxes; a similar approach could be followed for pervaporation, although other, more complex transport equations would be required for pervaporation, and typical time lag effects would not be seen.

One of the main drawbacks of all membrane techniques is lack of information necessary to fully understand and determine the transport mechanism [24]. Although pervaporation is considered to be one of the best understood processes, there are still many uncertainties. Additionally, according to the literature, it is not yet clear whether solution-diffusion model can be applied in the same way for unfilled and filled membranes. Therefore the necessity of further research by taking into account wider range of experimental parameters (i.e. variety of membranes, feeds, experimental conditions) is of high importance from the modeling point of view. For example, Baker approach [25] was found to be useful to derive the important equations for describing mass transport in pervaporation, when swelling and coupling effects due to swelling are negligible. The basis for transport description is Fick's law:

$$J_i = -D_i \cdot \frac{dc_i}{dx} \quad (1)$$

where D_i represents the diffusion coefficient of component i , and dc/dx the concentration gradient over the membrane. After applying several assumptions, Eq. (1) can be written into the following form:

$$J_i = \frac{P_i^G}{l} (p_{i,0} - p_{i,l}) = \frac{P_i^G}{l} (c_i H_i - p_{i,l}) \quad (2)$$

where P_i^G is the permeability coefficient, c_i the feed concentration, H_i the Henry coefficient, $p_{i,0}$ and $p_{i,l}$ the partial pressures at the feed and permeate side respectively of component i and l the membrane thickness.

In the ideal case, according to Eq. (2), the partial flux should increase linearly with increasing feed concentration and increasing partial pressure difference. Unfortunately, the influence of these two parameters on the membrane selectivity is not as straightforward as for the partial flux. In general, the selectivity is expected to decrease with increasing concentration of the faster permeating components in the feed, due to the swelling phenomenon. The effect of the permeate pressure on the selectivity depends on the relative volatilities between the components in the mixture [26].

This work focuses on the detailed study of silicalite filled and unfilled laboratory-made PDMS membranes performance in pervaporation of ethanol/water mixtures with different concentrations of alcohol in the feed and at various temperatures. In this way the applicability of the solution-diffusion model was examined for filled membranes in comparison with unfilled ones. Two different types of fillers were incorporated into the PDMS network: commercial ZSM-5 fillers (CBV 3002) and laboratory-made 'colloidal silicalite-1' in order to examine their influence on the process performance. Since it was not the aim of this study to investigate the effect of filler concentrations, recommended values from the literature [27] were applied. Additionally, the effect of membrane swelling on membrane performance parameters, such as total flux, partial fluxes and selectivity was examined by testing both unfilled and filled PDMS membranes. Obtained results were then compared with performance parameters obtained for novel block co-polymer based porous and dense SBS membranes.

2. Materials and methods

2.1. Membranes

In this study laboratory-made unfilled (M1), CBV 3002 filled (M2) and silicalite-1 filled PDMS (polydimethylsiloxane) membranes on a PI (polyimide) support and SBS (styrene-butadiene-styrene) block co-polymer membranes (M4 and M5) were used. The procedure of membrane preparation is described below.

2.1.1. PDMS membranes

The polyimide (PI) support layer was prepared first by casting a solution of Matrimid 5218 (Huntsman, Switzerland) on a polypropylene non-woven FO 2471, kindly provided by Freudenberg (Germany). A PI-solution, consisting of 15 wt.% PI, 2 wt.% H₂O, 62.25 wt.% NMP and 20.75 wt.% THF was cast on the non-woven support with a knife blade, set at a gap of 250 µm. After casting, evaporation of the solvent for 30 s was applied to ensure formation of the skin layer with elevated polymer concentration. This prevents intrusion of PDMS into the support pores during subsequent dip coating [13]. The resulting film was then immersed in water at room temperature to form the membrane.

After immersion precipitation, membranes were placed for 24 h in a crosslinking mixture (paraxylendiamine/methanol 1 g: 10 ml), as proposed by Vanherck et al. [28], and then rinsed with methanol in order to remove all traces of the reactant. Support was further treated by a solvent-exchange procedure, involving immersion in isopropanol (IPA) for 3 h and subsequently for 3 days in a mixture of toluene/4-methyl-2-pentanone/lube oil with volume ratio of 40:40:20. Obtained films were then wiped with tissue and dried in the oven at 60 °C for at least 1 h.

A PDMS (General Electrics, RTV 615A and B, respectively pre-polymer and cross-linker in a 10:1 ratio) in hexane was pre-polymerized at 60 °C for 0.5 h, followed by mixing for 0.5 h at room temperature. To coat the solution on the PI support, the support was taped onto a stainless steel plate, which was placed under an angle of 60° to allow the polymer solution to flow down over the support. After a part of solvent has evaporated, the plate was turned upside down and the coating procedure was repeated. After evaporation of most of the solvent, the membrane was placed in an oven for at least 1 h at 110 °C to complete crosslinking and to evaporate all traces of solvent. The concentration of all PDMS solutions was 10 wt.%.

Two types of fillers were used to prepare filled PDMS membranes: laboratory-made 'colloidal silicalite-1' and commercially available silicalite zeolite fillers (CBV 3002). Colloidal silicalite-1 is characterized by a particle size between 100 and 230 nm and is synthesized according to Ravishankar et al. [29]. Commercial CBV 3002 fillers are characterized by a particle size ranging from 1 to 1.5 µm and a Si/Al ratio of 240.

Zeolite filled PDMS membranes were prepared by following the procedure described by Gevers et al. [30]. The filler fraction was expressed in weight percent:

$$\text{filler fraction} = \frac{(\text{weight of filler})}{(\text{weight of filler}) + (\text{weight of polymer})} \times 100 \quad (3)$$

The filler content in the membrane was either 15 or 30 wt.%, for silicalite-1 and CBV 3002 fillers, respectively. This choice was based on the information given by Moermans et al. [27], where the nano-sized zeolites were found to show much improved pervaporation results in terms of membrane performance compared with micron-sized silicalite membranes. Hence, in order to test membranes with expected comparable performances, different

loadings have been applied for silicalite-1 and CBV 3002 fillers. The PDMS/filler solutions were coated on the PI support by following the procedure described above.

2.1.2. SBS membranes

Two types of SBS membranes were prepared: dense and symmetric structure (M5) obtained by solvent evaporation, and open and asymmetric membrane (M4) prepared by applying phase inversion, as described in the US Patent 2008/0114087 [31].

2.2. Membrane characterization

2.2.1. Contact angle measurement

The standard procedure of contact angle measurements is to put a drop on the top layer of a membrane and to examine the contact angle with a special camera. Measurements were done with water by using CAM 100 (KSV Instruments, Ltd.).

2.2.2. Scanning Electron Microscopy (SEM)

Membrane cross-sections were obtained by breaking the membranes under liquid nitrogen. Measurements of the membrane thickness were done by means of Scanning Electron Microscope (Cambridge Instruments Stereoscan 360) at 20 kV.

2.3. Pervaporation set-up

The dead-end pervaporation unit used in the experiments is described elsewhere [7]. During pervaporation, vacuum was applied on the permeate side and maintained constant (1 mbar) to ensure driving force for the separation. The active membrane area was 8.81 cm².

Experiments were carried out with ethanol/water mixtures, with alcohol concentration ranging from 3 to 9 wt.%. This concentration range was found to be a good representation of ethanol concentration in the feed used by other researchers in the pervaporative separation of alcohol/water mixtures [18,19,27,32,33], what allows reader better comparison of membrane performance. Constant stirring of the feed was applied in order to avoid concentration polarization. The effect of temperature was also examined by changing the range from 41 up to 61 °C. Tsuru et al. [34,35] and Machado et al. [36] also studied this effect and stated that the overall temperature dependency of the flux follows an Arrhenius type of relation:

$$J = J_0 \exp\left(-\frac{E_j}{RT}\right) \quad (4)$$

where T is the temperature, R the gas constant, and E_j is the activation energy of the flux relation, which can be expressed as a combination of the activation energy of diffusion E_D , the heat of adsorption ΔH_S and the heat of vaporization ΔH^{vap} :

$$E_j = E_D - \Delta H_S + \Delta H^{vap} \quad (5)$$

Bettens et al. [37] suggested that the transport is often described in terms of the membrane thickness normalized permeability coefficient F ,

$$F = \frac{J}{\Delta P} = \frac{SD}{L} = \frac{S_0 D_0}{L} \exp\left(\frac{\Delta H_S - E_D}{RT}\right) \quad (6)$$

where ΔP stands for the transmembrane partial pressure difference, S_0 is the adsorption coefficient at reference temperature, D_0 represents the diffusion coefficient at reference temperature and L is the membrane thickness. This allows expressing the activation energy of permeability as the difference between the activation energy of diffusion (E_D) and the heat of adsorption (ΔH_S). The

difference in activation energy of flux and permeability is caused by the temperature dependency of the driving force ΔP .

On the basis of Eq. (6), activation energy of permeability can be calculated from the linear regression of $\ln F$ as a function of the reciprocal temperature. As stated by Bettens et al. [37], depending on the fact whether the transport activation energy exceeds the heat of adsorption or not, both positive and negative values of E_F can be obtained.

Permeate was collected as a function of time in glass container using liquid nitrogen in a flask as a cooling trap. The concentration of ethanol in the permeate samples was determined using refractometer (Abbe 60 IDR). Total flux was calculated using Eq. (7) and normalized by the membrane thickness.

$$J = \frac{m}{A \cdot t} \quad (7)$$

m , mass of the sample (kg); A , active membrane area (m²); t , collection time (h).

Partial fluxes were calculated on the basis of the components concentration in the permeate obtained during quantitative analysis.

Selectivity of the membrane was calculated as follows:

$$\alpha = \frac{\left(\frac{x_A}{x_B}\right)_{\text{permeate}}}{\left(\frac{x_A}{x_B}\right)_{\text{retentate}}} \quad (8)$$

where x is a molar fraction, A represents the preferential component (ethanol) and B stands for water.

3. Results and discussion

3.1. Membrane characterization

Table 1 presents data on the membrane characterization.

All membranes used in this research showed similar values of contact angles measured with water ($\sim 117^\circ$), which proves the high hydrophobicity degree of the membrane material. The identical hydrophobicity of examined PDMS and SBS membranes gives a good basis for comparison of the membranes performance. Thickness of the membranes measured by means of SEM varied depending on the membrane structure (addition of the fillers, membrane material, etc.).

Composite PDMS/PI membranes were characterized by the highest total thickness ($\sim 90 \mu\text{m}$) in comparison to novel SBS membranes, either porous or dense (77 and 34 μm respectively). When the structures of composite PDMS and non-composite SBS membranes are being compared, and therefore the transport limitations are taken under consideration, it is important to highlight that for non-composite SBS membranes, the total cross-section is responsible for the separation process, while in case of composite materials only the dense (selective) top layer determines the separation.

Table 1
Characteristics of PDMS-based and SBS membranes used in the experiments.

Membrane	Composition	Contact angle (°)	Thickness (μm)	
			Total	Top layer
M1	PDMS/PI	114	91.9	12.5 ± 2
M2	CBV 3002 filled PDMS/PI	116	94.5	20.5 ± 4
M3	Silicalite-1 filled PDMS/PI	117	99.5	20.5 ± 4
M4	Porous SBS	119	77.7	–
M5	Dense SBS	115	34	34

Hence, the SBS membranes are characterized by a larger separation area, in comparison to examined PDMS membranes.

Additionally, incorporation of the fillers into the PDMS network led to almost double increase of the top layer thickness (from 12.5 to 20.5 μm for unfilled and filled PDMS membranes, respectively). The selective layer thickness did not depend on a concentration of the fillers in the polymeric network. At this point, it is however difficult to explain this result, since literature on the unsupported PDMS membranes proves an increase of selective layer thickness with incorporation of higher filler loadings [18,27].

Membrane structures are presented in Fig. 1a–e. As can be seen from Fig. 1, PDMS composite membranes consisting of PI support were characterized by an open structure with finger-like pores coated by a dense PDMS top layer. Between support and top layer a thin skin layer is clearly visible, what prevented the PDMS intrusion into the PI pores during coating procedure. Image D presents open and asymmetric structure of SBS membrane with sponge-like structure, in contrary to dense and symmetric morphology obtained from the same polymeric material via evaporation (image E).

3.2. Pervaporation

3.2.1. Effect of time

Fig. 2 presents the total permeate flux plotted as a function of time for water/ethanol mixture containing 6 wt.% of alcohol at different temperatures through M1.

As can be seen, the total flux generally decreases with time during the experiment. A sharp total flux decrease was observed during the first hour of pervaporation, when the feed temperature was maintained constant at 41 $^{\circ}\text{C}$, in contrast to the other experimental data, what is related with the method of carrying out the experiments. In this research, a temperature of 41 $^{\circ}\text{C}$ was considered as a starting point. After reaching the set point, which was controlled at the pervaporation module, vacuum was applied on the permeate side causing a sudden change of conditions (i.e. change in the driving force). From that moment, concentration of the selective component (alcohol) in the feed is decreasing with experimental time. As time goes on, the steady-state is being reached, leading to a slower decrease of the alcohol concentration, in comparison to non steady-state conditions. On one side it is related with a lower

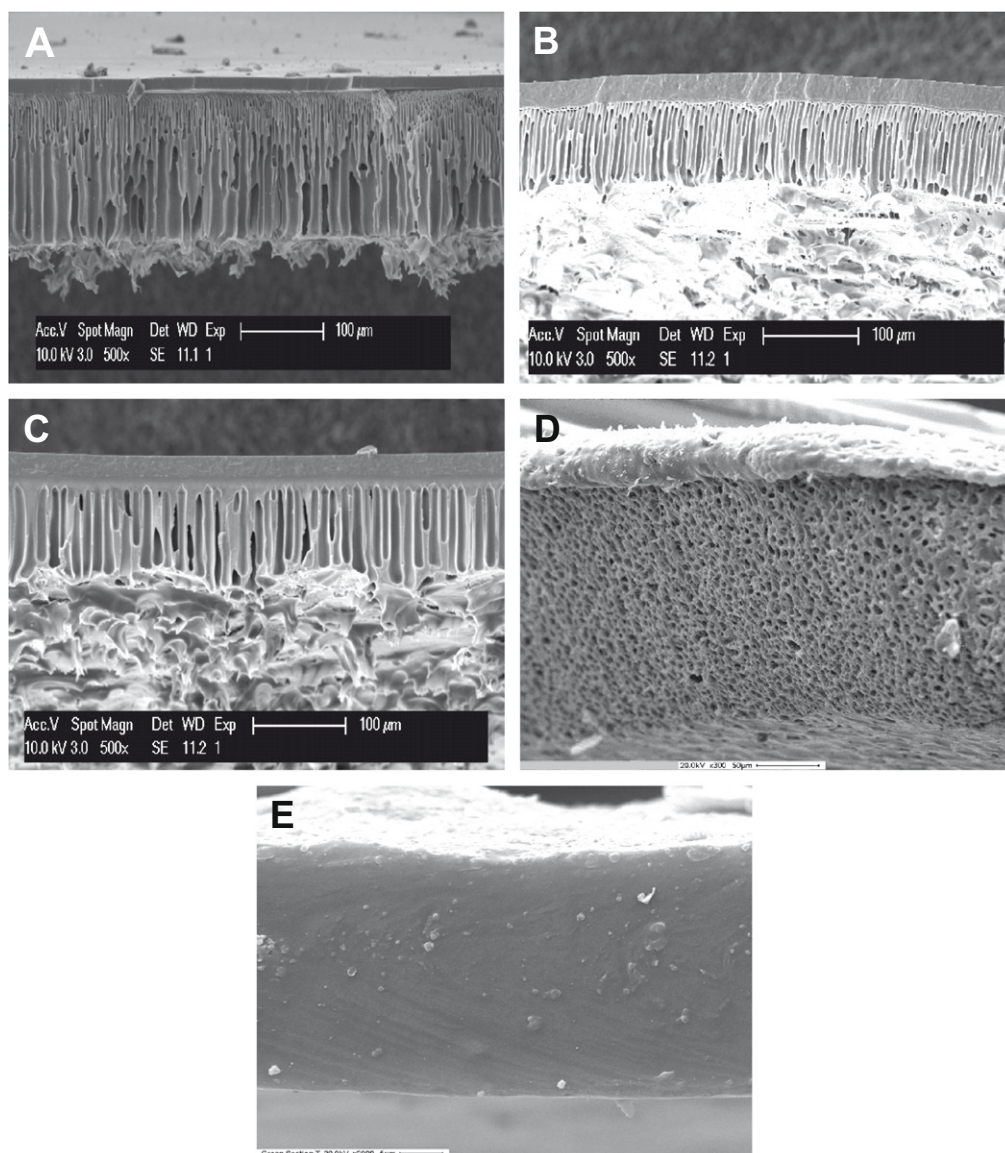


Fig. 1. Cross-sections of membranes used in the experiments taken by means of SEM (A – unfilled PDMS/PI, B – PDMS/PI filled with commercial CBV 3002, C – PDMS/PI filled with colloidal silicalite-1, D – porous SBS, E – dense SBS).

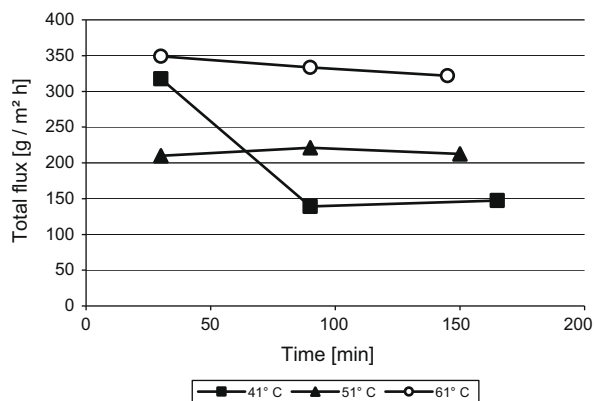


Fig. 2. Time dependency of the total permeate flux through membrane M1, concentration of ethanol in the feed: 6 wt.%, pressure: 1 mbar.

alcohol concentration in the feed as a consequence of partial transportation of the selective component before equilibrium was reached, but on the other hand with an increase of the mass transfer resistance in boundary layer. The steady-state was reached after approximately 90 min from the start of the experiment. After collection of steady-state samples, certain amount of ethanol (calculated by mass balance) was added to the feed tank in order to start experiment with equal feed concentration, and followed by raise of temperature up to 51 °C, allowing next measurement. Here, a lower decrease of the flux with time was observed, due to the fact that membrane was already 'pre-conditioned' by a vacuum.

These results were representative for all ethanol/water mixtures examined and all membranes used, and correspond well with data obtained by Mohammadi et al. [38] and Li et al. [39].

3.2.2. Effect of the feed composition

Total flux data as a function of ethanol concentration in the feed for PDMS-based membranes used in the experiments carried out at 41 °C are presented in Fig. 3.

As can be seen, all the examined mixtures follow roughly the same trend: a steady-state increase of the total flux with increasing alcohol fraction in the feed. For all examined temperatures, the highest increase in the total flux (i.e.: ~45% at 41 °C) was obtained for M3 when the concentration of the feed increased from 3 to 9 wt.%, while the lowest increase (~ 25% at 41 °C) was observed for unfilled membrane M1.

In order to determine transport through examined membranes, plots of ethanol flux and water flux versus ethanol concentration in the feed at 41 °C were prepared (Figs. 4 and 5).

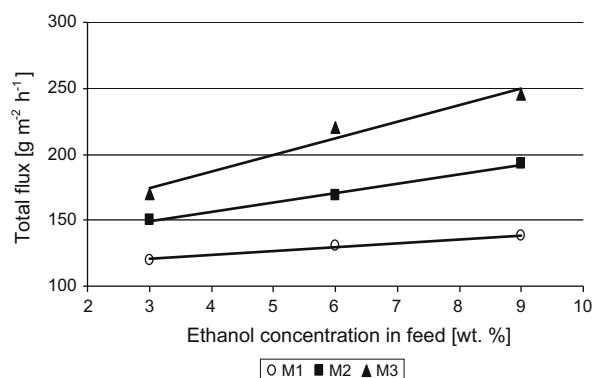


Fig. 3. Effect of the feed ethanol concentration on the total flux measured at 41 °C through M1, M2 and M3 membranes, pressure: 1 mbar.

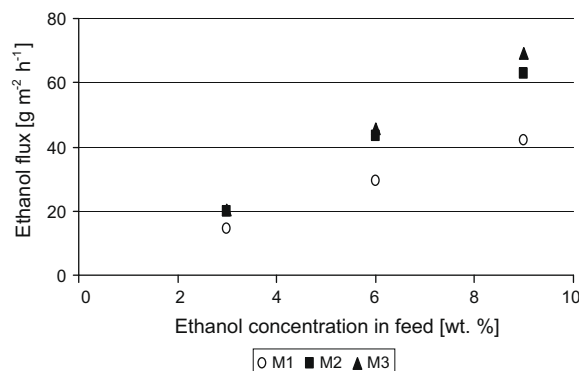


Fig. 4. Effect of feed ethanol concentration on the ethanol flux measured at 41 °C through M1, M2 and M3 membranes, pressure: 1 mbar.

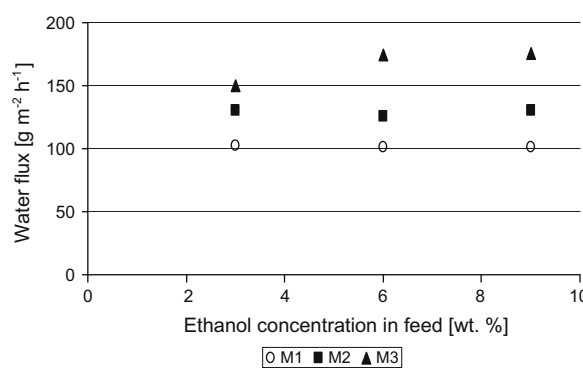


Fig. 5. Effect of feed ethanol concentration on the water flux measured at 41 °C through M1, M2 and M3 membranes, pressure: 1 mbar.

According to the solution-diffusion model (Eq. (2)), partial flux of component i is directly proportional to the permeability coefficient of component i and its partial vapor pressure difference between both sides of a membrane. Since P_i^G is defined as a product of diffusion and sorption coefficients of component i , hence any change in the feed composition is expected to directly affect the sorption phenomena at the liquid membrane interface. Additionally, the diffusion of mixture components and their solubility is dependent on the feed concentration [10]. From the analysis of the plots presented in Fig. 4, the conclusion can be drawn that increase of the ethanol concentration in the feed significantly increased the partial flux of ethanol for all tested membranes. The highest increase in ethanol flux, and comparable with values measured for M2, was obtained when membrane M3 was tested. Here, increase of the feed concentration from 3 to 9 wt.% caused increase of the ethanol flux by a factor 3.6, next to triple increase in the ethanol flux observed for M1. This increase could be explained by the increasing ethanol sorption into the membrane, which consequently resulted in membrane swelling. On the other hand, the increase of ethanol concentration in the feed did not influence the water flux, which remained constant within the examined alcohol concentration range. This result is in contrast with the solution-diffusion model, according to which the water flux is expected to decrease with the ethanol concentration in the feed increase. A possible explanation for this might be a relatively small change in the percentage of water content in the mixture, which varied between 97 and 91 wt.%. In the case of separations where higher concentrations of ethanol in the feed are applied, simultaneous increase of ethanol content in the permeate, next to decrease in separation factor, are typically observed. This was proven by Chen

et al. [40] who investigated the performance of unsupported filled silicone rubber membranes in the separation of ethanol/water mixtures containing between 4 and 91 wt.% of ethanol in the feed. The authors observed that ethanol content in the permeate increases drastically at low feed concentrations, resulting in the high separation factors (28.5 for ethanol/water mixture containing 4 wt.% of ethanol in the feed), whereas separation factor decreases drastically at higher ethanol concentrations in the feed (separation factors of 7.7 and 2.3 in the case of mixtures containing 26 and 91 wt.% of ethanol, respectively), due to an extensive swelling of PDMS rubber. By taking into account above considerations, the assumption can be made that the alcohol flux was primarily influenced by its own gradient in chemical potential, and not by the water permeation, what also corresponded with hydrophobicity degree of the PDMS materials.

In order to investigate the swelling effect in more detail, pure water and pure ethanol permeation experiments were carried out at 41 °C (Table 2). Analysis of the data presented in Table 2 confirms the conclusion that increase of ethanol concentration in the feed significantly influences the permeate flux. As presented in Fig. 3, change of the ethanol concentration from 3 to 9 wt.% led to a linear increase in the total flux, whereas a more pronounced increase in the total flux was observed when pure ethanol was used as a feed. Moreover, it was found that swelling does not occur when pure water is applied, since the lowest total flux values were obtained for all tested membranes. The highest swelling effect was observed for the unfilled M1 membrane in comparison to filled M2 and M3 membranes. Here, increase of the ethanol concentration in the feed from 0 to 6 wt.% resulted in only a double increase of the total flux, followed by an increase in total flux by a factor of 27, when the ethanol concentration in the feed increased to 100 wt.%. Among filled PDMS membranes (M2 and M3), the influence of the PDMS swelling was found to be the lowest in the case of M2. For these membranes, a similar increase in the total flux was observed for the concentration range 0–6 wt.% in comparison to M1, whereas increase of the feed concentration up to 100 wt.% leveled total flux 13 and 17 times for M2 and M3, respectively. On the basis of above considerations, the conclusion can be drawn that application of pure ethanol maximizes the effect of swelling, while incorporation of the fillers plays an important role in the reduction of this side effect.

Opposite findings for PDMS membranes were reported by Mohammadi et al. [38], where water flux increased significantly with an increase of selective component concentration in the feed in comparison to alcohol flux. The authors stated that increase in the membrane-free volume and thus simultaneous increase of

the side chain mobility, caused by the feed concentration increase allowed easier permeation of the small-sized water clusters through the membrane-free volume, leading therefore to enhanced water diffusion. In this work the highest water flux was obtained for M3 ($\sim 167 \text{ g m}^{-2} \text{ h}^{-1}$ at 41 °C), while the lowest was obtained in case of the M1 membrane ($\sim 100 \text{ g m}^{-2} \text{ h}^{-1}$). The water flux measured through membrane M2 was found to be more in the range of values obtained for M1, than M3 ($\sim 128 \text{ g m}^{-2} \text{ h}^{-1}$).

From the above considerations it can be expected that an increase in the alcohol concentration in the feed will also influence the selectivity of the membranes, since a significant increase in ethanol (selective component) flux and a constant water flux were found. Fig. 6 presents this effect.

The selectivity of all examined membranes is strongly dependent on the alcohol content in the feed. Higher concentration of organic (selective) compound in the feed led to decrease in membrane selectivity. The highest decrease was observed for membrane M3 in comparison to M1 and M2. In case of M1 effect of the feed concentration on the selectivity was the least pronounced. From analysis of the data presented in Figs. 4 and 5, it can be seen that M3 membrane showed additionally the highest water flux among other PDMS membranes examined, and moreover ethanol flux comparable with membrane M2. Hence the conclusion can be drawn, that, in case of M3, membrane incorporation of fillers into the PDMS network did not influence the membrane swelling, leading to increasing polymer chains mobility with the ethanol concentration in the feed increase and therefore increased free volume available for permeation. That made the membrane structure more open, allowing easier permeation of all components, and thus resulted in a higher concentration of non-preferentially permeating components in the permeate. The opposite findings were clearly visible for M2 membrane, where incorporation of silicalite zeolite fillers led to a significant increase of ethanol flux and less pronounced increase of water flux, which was comparable with unfilled M1 membrane. The above observations allowed concluding that, for membrane M2, swelling effect was significantly reduced, since also calculated selectivities were the highest. This result corresponds well with data obtained by Vankelecom et al. [19], where crosslinking effect of zeolites was found and led to reduced membrane swelling. At this point it is not possible to explain the difference between crosslinking effects of fillers in M2 and M3, due to the lack of crosslinking density data for prepared membranes. This inconvenience is a consequence of the rather ill-defined structure of RTV 615 components used in the PDMS synthesis.

Jia et al. [18] found that silicalite filled membranes do not show an improved performance if the zeolite crystals are not dispersed homogeneously in the polymer. Additionally, observation was made that the aggregates of zeolite crystallites often form pinholes,

Table 2

Comparison of ethanol concentration in the feed effect on the total flux obtained for PDMS-based membranes (M1, M2 and M3).

Membrane	C_{EtOH} (wt.%)	Total flux ($\text{g m}^{-2} \text{ h}^{-1}$)
M1	0	63.7
	3	120.1
	6	130.7
	9	138.0
	100	3550.2
M2	0	54.5
	3	150.4
	6	169.0
	9	193.0
	100	2354.0
M3	0	83.9
	3	170.0
	6	220.2
	9	245.0
	100	3029.0

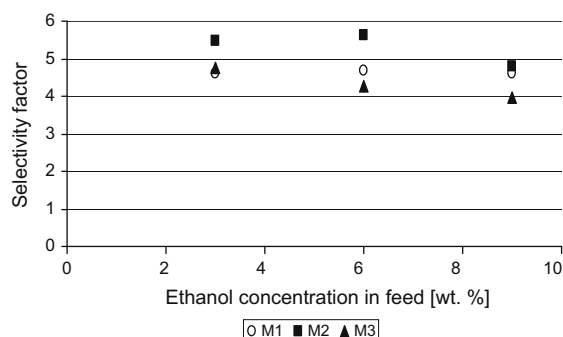


Fig. 6. Effect of feed ethanol concentration on selectivity measured at 41 °C through M1, M2 and M3 membranes, pressure: 1 mbar.

which can lead to lower selectivity in comparison to the corresponding pure polymer membranes. According to the authors, an increase of the silicalite concentration in the polymeric network results in a reduction of membrane swelling and moreover, in formation of a pinhole-free membrane what improves the mechanical strength of the active layer. Moermans et al. observed a similar effect [27], namely the best performance results obtained for PDMS membranes with the highest (40 wt.%) silicalite loading in the polymer. As stated by the authors, the higher concentration of zeolites incorporated into the network, the less swelling. Moreover, selectivity and flux were found to improve significantly when nano-sized zeolites were applied in comparison to micron-sized ones. Results obtained in this research confirm above considerations, showing that size of the particles and concentration of the filler play an important role in separation, since good filler dispersion was obtained for larger CBV 3002 fillers (Fig. 7A) in contrary to silicalite-1 fillers, where formation of particle agglomerates with size of 1–5 μm was clearly visible (Fig. 7B).

3.2.3. The temperature effect

The effect of the temperature on the total and partial fluxes for 3 wt.% ethanol/water mixture is presented in Figs. 8–10.

Increasing working temperature caused a significant increase in the total permeate flux. A similar effect was observed by Mohammadi et al. and Sampranpiboon et al. [38,41]. The authors stated that during pervaporation permeating molecules diffuse through free volumes of the membrane. Thermal motions of polymer chains in amorphous regions randomly produce free volumes. As temperature increases, frequency and amplitude of polymer jumping chains increases. Thus, at higher temperatures, the diffusion rate of individual permeating molecules increases leading to high permeation fluxes. In this work, comparable increase in the total flux was observed for all tested membranes (2.42, 2.58 and 2.71 for M1, M2 and M3 respectively). As mentioned in Section 3.2.2, the permeate flux through PDMS composite membranes increased with increasing concentration of ethanol in the feed, due to the swelling effects.

In order to get insight into the temperature effect on the swelling phenomena, additional experiments were carried out with water and pure ethanol by varying the temperature of permeation (Figs. 11 and 12) for all PDMS membranes.

As can be seen in Figs. 11 and 12, the swelling was more promoted in the case of pure ethanol, in comparison to water. For example, in the case of M2 membrane, the same temperature effect was found for water and pure ethanol permeation, resulting in the increase of the total flux by a factor of 2. Whereas for M3, higher increase in the total flux for permeation of ethanol was observed (factor 2.2), while in the case of water permeation the total flux changed only 1.5 times. For example, in case of M2 increase of the experimental temperature increased pure water permeation by a factor of 1.5, whereas more pronounced effect was clearly visible

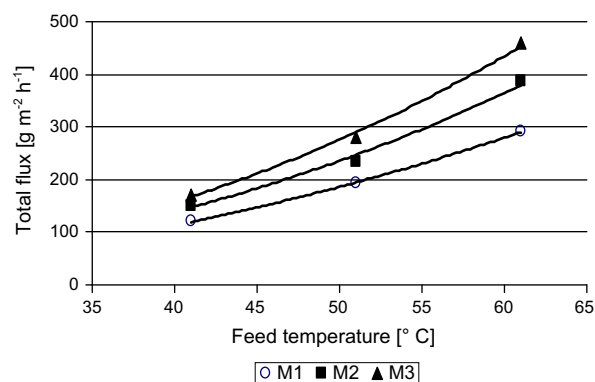


Fig. 8. Comparison of temperature dependency on the total flux for 3 wt.% ethanol/water mixture through M1, M2 and M3 membranes, pressure: 1 mbar.

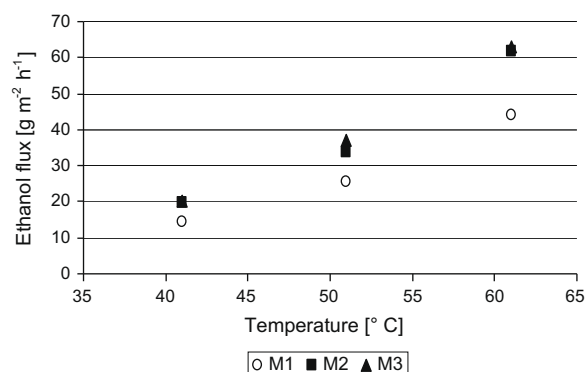


Fig. 9. Comparison of temperature dependency on the ethanol flux for 3 wt.% ethanol/water mixture through M1, M2 and M3 membranes, pressure: 1 mbar.

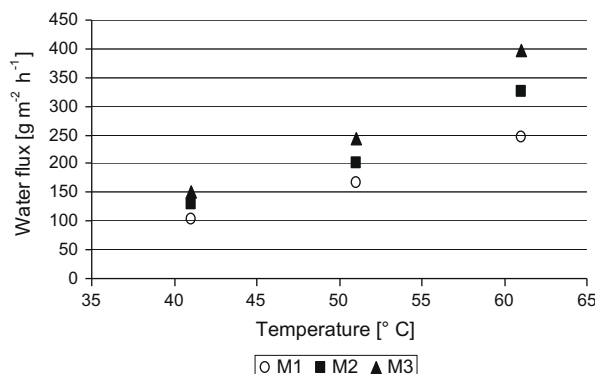


Fig. 10. Comparison of temperature dependency on the water flux for 3 wt.% ethanol/water mixture through M1, M2 and M3 membranes, pressure: 1 mbar.

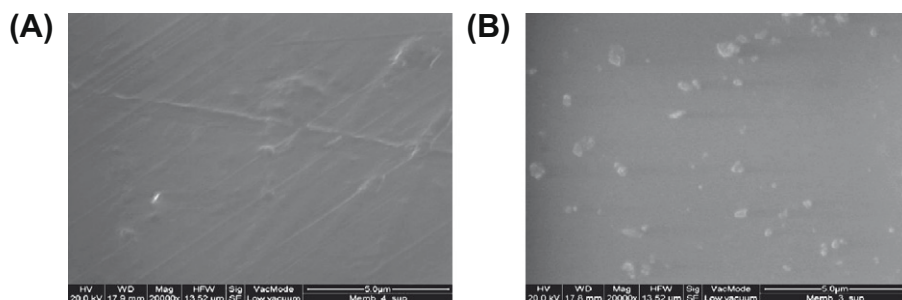


Fig. 7. SEM images of CBV 3002 (A) and silicalite-1, (B) fillers dispersion in the PDMS network.

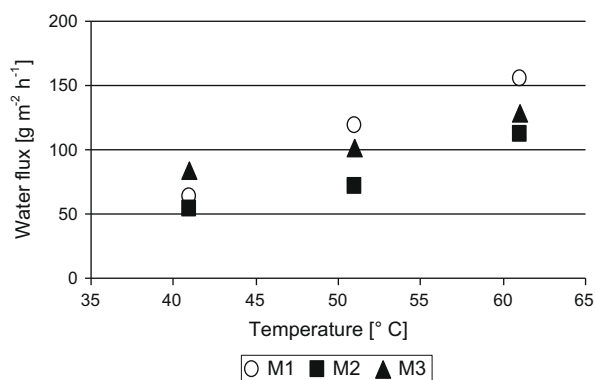


Fig. 11. Temperature dependency on the water flux obtained during permeation of pure water for PDMS-based membranes (M1, M2 and M3).

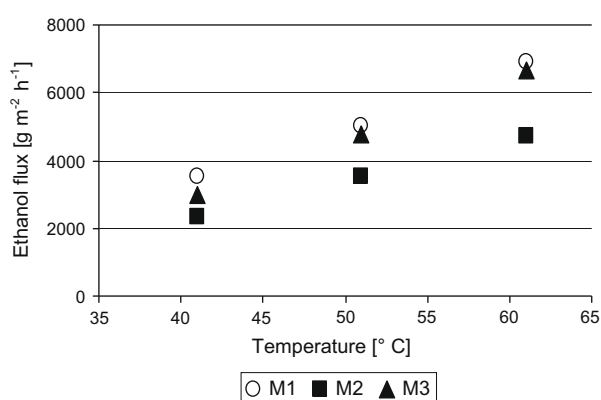


Fig. 12. Temperature dependency on the ethanol flux obtained during permeation of pure ethanol for PDMS-based membranes (M1, M2 and M3).

ible when ethanol was applied as a feed (increase of ethanol flux by a factor of 2.2). Comparison of results obtained for M1 led to conclusion, that effect of temperature on the water permeation was the highest among all PDMS-based membranes examined (total flux increased 2.5 times), next to comparable results obtained for ethanol permeation. Obtained results again confirm that incorporation of the silicalite fillers reduces swelling phenomena. Moreover, this effect was also more pronounced for M2 in comparison to M3. Additionally, on the basis of above, it can be noted that an increase of the separation temperature was found to promote swelling phenomena. This conclusion is in a good agreement with observations made by Vane et al. [42] for separation pervaporative removal of ethanol from ethanol/water mixtures containing 5 wt.% of alcohol through unsupported filled (silicalite-1 and CBV 28014) PDMS membranes at elevated temperatures (30–70 °C). According to the authors, higher temperatures can possibly increase the total flux, but at the same time may not deliver expected increase in the membrane selectivity, what corresponds well with results obtained by Klein and Abraham [43], proving a decrease in the amount of ethanol sorbed by silicalite fillers with increasing temperature. The temperature dependence of the flux suggests that pervaporative transport through examined PDMS-based membranes was an activated process.

Bettens et al. [37] studied also the effect of size parameters on the alcohol and water flux through tubular microporous silica membranes, since molecular size is expected to influence diffusion, as suggested by the Stokes–Einstein equation. In their work, the flux increase with decreasing molecular weight and decreasing kinetic diameter was found, when the working temperature was maintained below 50 °C. Above this temperature, no correlation

between molecular size and flux was observed, hence the conclusion could have been drawn that sorption effects are dominant over diffusion effects and thus rate determining for the mass transport. In this study, higher increase of ethanol flux with increasing temperature in comparison to water flux was observed (i.e. in case of the M2 membrane ethanol flux increased 3.2 times, while water flux only 2.5 times). Since ethanol is characterized by a bigger size (effective diameter of 0.733 nm) than water (effective diameter of 0.323 nm), the assumption can be made that the diffusions effects are dominant over the sorption effects, and thus are expected to be the determining parameter in the transport mechanism description through PDMS-based membranes. Additionally from the data presented in Figs. 9 and 10 it can be seen that the highest increase of ethanol and water flux with temperature was obtained for filled M2 and M3. Moreover, membrane M3 was characterized by a higher increase of the water flux in comparison to M2, while the equal influence of temperature on ethanol flux was found for these membranes.

Moermans et al. [27] highlighted that nano-sized zeolites in PDMS have a remarkable effect on the pervaporation of ethanol–water mixtures, what was related with presence of the mesopores in the silicalite-1 samples. According to the authors, these mesopores arise due to the voids between the nanocrystals and are expected to act as freeways for the preferentially sorbed ethanol. In this work, loading of silicalite-1 fillers in PDMS network was lower in comparison to [27], therefore better dispersion and hence better pervaporation results were obtained when larger and easier to disperse CBV 3002 fillers were applied.

From the data presented in Fig. 13, an increase in selectivity with increasing temperature was observed, but on the other hand, the selectivity decreased with the ethanol concentration.

Liang et al. [44] also observed this effect and explained it by temperature dependent decrease of the hydrogen bonding between water and alcohol molecules. When that happens, then less water is stimulated to permeate through the membrane, which is more selectively swollen by ethanol. If swelling was a dominant effect in transport through pervaporation membranes, decrease of the membrane selectivity with temperature increase would be expected. In contrary, the selectivity increase with increasing temperature was found. The highest increase in selectivity with increasing temperature for a mixture containing 3 wt.% of ethanol was observed in case of the M1 membrane, where selectivity increased by a factor 1.4. For this membrane the influence of ethanol concentration in the feed was also less pronounced. Moreover, decrease of the temperature dependency on the selectivity with ethanol concentration increase was observed. For membranes M2 and M3 this effect was not seen, and the increase in the selectivity remained constant (~1.2 and 1.1 times for M2 and M3 respectively). Additionally, increase of temperature led to lower increase in

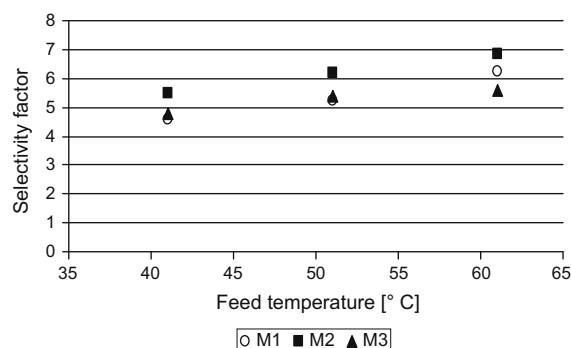


Fig. 13. Comparison of temperature dependency on selectivity flux for 3 wt.% ethanol/water mixture through M1, M2 and M3 membranes, pressure: 1 mbar.

membrane selectivity in comparison with M1. The highest selectivity values were obtained for M2, what was an expected seen, since this membrane showed lower water flux, but on the other hand comparable ethanol flux in comparison to M3. Therefore, the conclusion can be drawn that crosslinking effect was more pronounced when commercial zeolite silicalite fillers were applied resulting in better membrane performance.

In Fig. 14 the straight-line correlation between the logarithm of permeability ($\ln F$) versus the inverse of absolute temperature is presented.

The activation energy of permeability (E_F) is found as the slope of the plotted line and the average values are presented in Table 3.

From the analysis of Fig. 14 it was clear that the solution-diffusion model was applicable to describe the transport through laboratory-made PDMS membranes. The temperature dependency of the fluxes suggested additionally that pervaporative transport through examined membranes is an activated process. The activation energy of permeability of both mixture components was positive. That implies that activation energies of diffusion E_D are larger than the respective heat of adsorption, what can be seen in Table 3. Moreover, higher values of activation energy for ethanol in comparison to water were obtained, what suggested that transport of ethanol was more activated. That was also visible in Figs. 4 and 5 where more rapid increase of the alcohol flux was observed with temperature than for the water flux. Vankelecom et al. [19] stated that the permeation of water through the membranes is always less activated than the permeation of the co-permeating alcohol. According to the authors, water is entrained by the alcohol through the membrane and the shorter the alcohol chain, the stronger this effect will be. The positive activation energies of permeability of both components are expected to be a result of substantial interactions with the pore wall upon diffusion, due to their high polarity. Additionally, the E_F differs from the activation values of the flux activation energy by the heat of vaporization. The highest activation energies of ethanol and water permeability were obtained for M2. In case of other filled membrane (M3), the activation en-

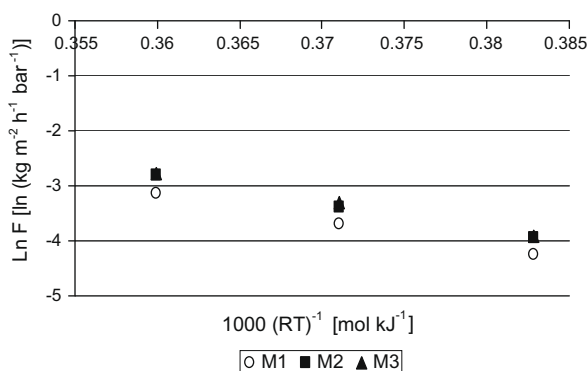


Fig. 14. Arrhenius plot of flux versus temperature for PDMS-based membranes (M1, M2 and M3).

Table 3

Activation energies for the permeation rate of ethanol/water mixtures.

Membrane	E_F (kJ/mol)		$-\Delta H_S$ (kJ/mol)	$E_D = E_F + \Delta H_S$ (kJ/mol)		$E_j = E_F + \Delta H^{vap}$ (kJ/mol)	
	EtOH	H ₂ O		EtOH	H ₂ O	EtOH	H ₂ O
M1	46.99	38.14	6.62	40.37	31.52	85.59	78.79
M2	49.73	40.09	10.83 ^b	38.90	29.26	88.33	80.74
M3	44.07	38.34	NA	–	–	82.67	78.99

NA – not available.

^a ΔH^{vap} for ethanol: 38.6 kJ/mol, for water: 40.65 kJ/mol [45].

^b Estimated value of ΔH_S based on data presented in [46].

Table 4

Performance of PDMS-based membranes and SBS membranes in ethanol removal from ethanol/water mixture containing 3 wt.% of alcohol at 41 °C.

Membrane	Flux (g m ⁻² h ⁻¹)			Selectivity α
	Total	EtOH	Water	
M1	120	14	106	4.6
M2	151	20	131	5.5
M3	170	20	150	4.8
M4	1943	190	1752	3.5
M5	146	21	125	5.5

ergy of alcohol permeability was found to be slightly lower than for unfilled membrane M1, whereas the activation energies of water permeability were comparable. This result suggests that pervaporative transport through membrane M2 is more activated process in comparison to M1 and M3. Additionally, lower activation energy is required to transport ethanol through M3 in comparison to M1. The data obtained in this work correspond well with results presented by Mohammadi et al. [38], where activation energy of ethanol through PDMS membranes was found to be 43.35 kJ/mol.

3.2.4. Performance comparison to SBS membranes

Hydrophobic pervaporation can be successfully applied in the industry as an environmentally friendly method of low-alcohol beverages processing and production of biofermentation products. In both processes the removal of alcohol is of major importance. Due to the increasing demand for membranes showing good performance, the development of new materials has become an interest of many researchers. In order to determine the efficiency of ethanol removal from ethanol/water mixtures, comparison of the membrane performances of PDMS-based membranes applied in this research was studied. Additionally, obtained membrane performances of PDMS-based membranes were compared with performance of novel SBS membranes, which showed good results in the removal of TCA from water [31].

Table 4 presents normalized total and partial fluxes obtained through examined membranes, together with membrane selectivity, measured at 41 °C for 3 wt.% ethanol/water mixture.

As can be seen from Table 4, the lowest total flux was obtained for the unfilled PDMS membrane. The incorporation of the fillers into the PDMS network caused an increase in the total flux, and at the same time increase of the ethanol flux. For example, the partial flux of ethanol through membrane M1 was estimated as 11.7% of the total flux, while incorporation of the fillers increased this up to 13.3% and 11.8% for M2 and M3 respectively. Moreover, membrane selectivity was found to be the lowest for unfilled membrane (M1). An increase in the selectivity in the case of filled PDMS membranes was considered as a result of two simultaneous effects: higher ethanol flux and constant water flux in comparison to M1.

While comparing the data obtained for M2 and M3, the conclusion can be drawn that the effect of fillers is more pronounced when 30 wt.% of commercial zeolite silicalite fillers was applied in comparison to PDMS filled with 15 wt.% of silicalite fillers, since

better membrane performance was obtained for the former (lower water flux ($131 \text{ g m}^{-2} \text{ h}^{-1}$) and the highest selectivity (5.5)). As stated earlier, this result is most likely due to inhomogeneous dispersion of smaller silicalite-1 fillers, resulting in formation of particle agglomerates, whereas this was not observed for M2 membrane.

Vankelecom et al. [19] also studied filled and unfilled PDMS membranes for removal of ethanol from ethanol/water mixture containing 6 wt.% of alcohol by pervaporation at 35°C . Lower values of the normalized total and partial fluxes in comparison to our data (for 3 wt.% of ethanol in water, 41°C) were reported. The authors additionally stated decrease in the total and partial fluxes for filled PDMS membranes in comparison to pure PDMS, what is in contrary with this research.

Newly developed SBS membranes showed comparable membrane performances to PDMS membranes. In case of M4, an outstandingly high total flux was observed ($\sim 1943 \text{ g m}^{-2} \text{ h}^{-1}$), what was related with highly porous structure of the membrane, in comparison to other membranes used. Moreover, the percentage of ethanol flux of total flux obtained through M4 ($\sim 9.8\%$) was lower in comparison to unfilled M1 ($\sim 11.7\%$), and the lowest selectivity was reached (3.5). M5, in contrary to M4, showed the best selectivity, next to membrane M2. The total and partial fluxes obtained through M5 were also comparable with fluxes obtained for M2, despite higher thickness of the dense layer.

As mentioned in the patent [31], the results obtained in terms of flux and selectivity of SBS membranes in TCA removal from water were significantly superior to those reported in the literature, where composite commercial PDMS-based membranes were applied. For example, at the concentration of TCA in water being 120 ppm, at 24°C and relatively high downstream pressure (40 Torr), the selectivity of 2000 was obtained, what was considered to be 2–3 times better than values gathered for commercial PDMS membranes. The authors also stated that, in case of SBS membranes, the influence of the permeate pressure on the partial flux of water and TCA is significant, and leads to more pronounced water flux decrease in comparison to TCA flux, resulting therefore in the selectivity increase. In this work however no attention was put on the effect of different permeate pressure in pervaporative removal of ethanol from ethanol/water mixtures examined. Therefore, higher selectivity of M5 (5.5), can be explained referring to the high affinity of SBS polymer towards organic molecules, such as TCE and TCA, which has been already described in literature [47]. In fact, considering the solubility parameter of SBS is about $17 (\text{J}/\text{cm}^3)^{1/2}$ and the solubility parameters for TCA and TCE are $17 (\text{J}/\text{cm}^3)^{1/2}$ and $18 (\text{J}/\text{cm}^3)^{1/2}$ respectively, while for water is $23 (\text{J}/\text{cm}^3)^{1/2}$ we can better understand the higher affinity of SBS towards the organic molecules than water. The same speculation can be also extended to SBS in contact with ethanol ($14 (\text{J}/\text{cm}^3)^{1/2}$) which also has higher affinity than water, even if not so strong as of TCA and TCE. In order to better understand the membrane-solvent interaction, swelling effect was also investigated by permeation of water and ethanol at 41°C (Table 5), as described for PDMS membranes. As can be seen from the data presented in Table 5, membrane M4 was found not to operate well in the contact with pure ethanol. A clear explanation for this is a significant swelling of membrane, resulting from the membrane-ethanol interaction. This effect determined a drastic increase of the membrane pore sizes available for permeation, making the membrane unselective and thus resulting in a high ethanol flux. As concerns M5, no significant influence of swelling on the total flux was found, since increase of ethanol concentration in the feed from 3 to 100 wt.% led to only double increase in the total flux, in comparison to PDMS-based membranes, as described before. This explains interesting membrane performance data obtained for M5.

As far as SBS membranes were proved to be characterized by better performances in the removal of TCA from water at low or-

Table 5

Comparison of ethanol concentration in the feed effect on the total flux obtained for SBS membranes (M4 and M5).

Membrane	C_{EtOH} (wt.%)	Total flux ($\text{g m}^{-2} \text{ h}^{-1}$)
M4	0	1864
	3	1943
	100	Not working
M5	0	104
	3	146
	100	310

ganic compound concentration, the selectivity and the fluxes in ethanol removal from ethanol/water mixtures at relatively higher concentrations seem to be comparable, despite the difference in the area of surface responsible for separation (dense top layer in case of PDMS materials and total surface of SBS materials). Hence, the conclusion can be drawn that the membrane structure plays an important role in the transport mechanism description when the separations at varying concentrations are examined (~ 10 wt.% and ~ 120 ppm). Therefore, detailed examination of temperature, pressure and incorporation of the fillers into the SBS membranes is to be carried out to fully understand the transport mechanism through these membranes.

4. Conclusions

It was found that the solution-diffusion model was a good representation of ethanol transport through both filled and unfilled PDMS membranes, whereas the water flux did not obey this model due to swelling effects. Membrane swelling was more pronounced in case of unfilled PDMS membranes, hence the conclusion was drawn that filler incorporation increased membrane stability by crosslinking. Increase of the temperature caused higher increase of ethanol flux in comparison to water flux, which was explained by a temperature related decrease of the hydrogen bonding between water and alcohol molecules. The membrane selectivity was strongly dependent on the feed concentration. A significant increase of the selectivity was observed for PDMS membrane filled with commercial CBV 3002 fillers, due to high ethanol flux and lower water flux obtained in comparison to nano-sized colloidal silicalite-1 filled membrane. Novel porous SBS membranes gave the highest ethanol fluxes, but membrane selectivity was rather low, in comparison to other membranes examined. On the other hand, the membrane performance of SBS membranes characterized by a dense structure was similar to the performance of filled PDMS membranes.

As concerns PDMS-based membranes further research is to be carried out to compare temperature and feed concentration effect on the membrane performance parameters for membranes containing the same amount of various fillers (15 and 30 wt.%). This will allow better understanding of role of filler type and its loading in the transport mechanism description. Addition of the fillers into SBS network may also provided very interesting data, what automatically becomes the objective of further examination, next to detailed investigation of process parameters influence on the membrane performance.

Acknowledgments

The K.U. Leuven Research Council is gratefully acknowledged for financial support (OT/06/37). I.F.J. Vankelecom acknowledges the Federal Government for an IAP-grant and the long term structural funding – Methusalem by the Flemish Government. The Erasmus Mobility program is also gratefully acknowledged for the

grant given to S. Chovau for performing the experimental work at ITM-CNR in Italy.

References

- [1] A.M. Polyakov, L.E. Starannikova, Yu.P. Yampolskii, *J. Membr. Sci.* 238 (2004) 21–23.
- [2] S.I. Semenova, H. Ohya, K. Soontarapa, *Desalination* 110 (1997) 251–286.
- [3] W.-H. Chan, C.-F. Ng, S.-Y. Lam-Leung, X. He, *Polymer* 39 (1998) 2461–2467.
- [4] X. Feng, R.Y.M. Huang, *J. Membr. Sci.* 109 (1996) 165–172.
- [5] K. Srinivasan, K. Palanivelu, A. Navaneetha Gopalakrishnan, *Chem. Eng. Sci.* 62 (2007) 2905–2914.
- [6] M. Vane, *J. Chem. Technol. Biotechnol.* 80 (2005) 603–629.
- [7] A. Verhoef, A. Figoli, B. Leen, B. Bettens, E. Drioli, B. Van der Bruggen, *Sep. Purif. Technol.* 60 (2008) 54–63.
- [8] A. Hasanoglu, Y. Salt, S. Keleser, S. Ozkan, S. Dinçer, *Chem. Eng. Process.* 46 (2007) 300–306.
- [9] M. Yoshikawa, T. Yoshioka, J. Fujime, A. Murakami, *J. Membr. Sci.* 178 (2000) 75–78.
- [10] B. Smitha, D. Suhanya, S. Sridhar, M. Ramakrishna, *J. Membr. Sci.* 241 (2004) 1–21.
- [11] H.L. Fleming, C.S. Slater, *Membrane Handbook*, Van Nostrand Reinhold, New York, 1992, p. 105.
- [12] R.Y.M. Huang (Ed.), *Pervaporation Membrane Separation Processes*, Elsevier Science Publishers, Amsterdam, 1991.
- [13] P. Vandezande, L.E.M. Gevers, I.F.J. Vankelecom, *Chem. Soc. Rev.* 37 (2008) 365–405.
- [14] T.C. Bowen, R.D. Noble, J.L. Falconer, *J. Membr. Sci.* 245 (2004) 1–33.
- [15] X. Lin, H. Kita, K. Okamoto, *Ind. Eng. Chem. Res.* 40 (2001) 4069–4078.
- [16] H. Matsuda, H. Yanagishita, H. Negishi, D. Kitamoto, T. Ikegami, K. Haraya, T. Nakane, Y. Idemoto, N. Koura, T. Sano, *J. Membr. Sci.* 210 (2002) 433–437.
- [17] S. Li, V.A. Tuan, J.L. Falconer, R.D. Noble, *Microporous Mesoporous Mater.* 58 (2003) 137–154.
- [18] M.-D. Jia, K.-V. Peinemann, R.-D. Behling, *J. Membr. Sci.* 73 (1992) 119–128.
- [19] I.F.J. Vankelecom, D. Depre, S. De Beukelaer, J.B. Uytterhoeven, *J. Phys. Chem.* 99 (1995) 13193–13197.
- [20] V.V. Tarabara, Multifunctional nanomaterial-enabled membranes for water treatment, in: N. Savage et al. (Eds.), *Nanotechnology Applications for Clean Water*, William Andrew Inc., 2009, pp. 59–75.
- [21] P. Meneghetti, S. Shaikh, S. Qutubuddin, S. Nazarenko, *Rubber Chem. Technol.* 81 (2008) 821–841.
- [22] T.-H. Bae, I.-C. Kim, T.-M. Tak, *J. Membr. Sci.* 275 (2006) 1–5.
- [23] H.S. Lee, S.J. Im, J.H. Kim, H.J. Kim, J.P. Kim, B.R. Min, *Desalination* 219 (2008) 48–56.
- [24] B. Bettens, J. Degreve, B. Van der Bruggen, C. Vandecasteele, *Sep. Sci. Technol.* 42 (2007) 1–23.
- [25] R.W. Baker, *Membrane Technology and Applications*, second ed., Kluwer Academic Publishers, 2003.
- [26] J. Neel, Q.T. Nguyen, R. Clement, D.J. Lin, *J. Membr. Sci.* 27 (1986) 217–232.
- [27] B. Moermans, W. De Beuckelaer, I.F.J. Vankelecom, R. Ravishankar, J.A. Martens, P.A. Jacobs, *Chem. Commun.* (2000) 2467–2468.
- [28] K. Vanherck, P. Vandezande, S.O. Aldea, I.F.J. Vankelecom, *J. Membr. Sci.* 320 (2008) 468–476.
- [29] R. Ravishankar, C.E.A. Kirschhock, P.P. Knops-Gerrits, E.J.P. Feijen, P.J. Grobet, P. Vanoppen, F.C. De Schryver, G. Miehe, H. Fuess, B.J. Schoeman, P.A. Jacobs, J.A. Martens, *J. Phys. Chem. B* 103 (1999) 4960–4964.
- [30] L.E.M. Gevers, I.F.J. Vankelecom, P.A. Jacobs, *J. Membr. Sci.* 278 (2006) 199–204.
- [31] S.K. Sikdar, J. Burckle, B.K. Dutta, A. Figoli, E. Drioli, US Patent 2008/0114087, 2008.
- [32] I.F.J. Vankelecom, J. De Kinderen, B.M. Dewitte, J.B. Uytterhoeven, *J. Phys. Chem. B* 101 (1997) 5182–5185.
- [33] B. Adnadjevic, J. Jovanovic, S. Gajinov, *J. Membr. Sci.* 136 (1997) 173–179.
- [34] T. Tsuru, M. Miyawaki, H. Kondo, T. Yoshioka, M. Asaeda, *Sep. Purif. Technol.* 32 (2003) 105–109.
- [35] T. Tsuru, T. Sudou, S.-i. Kawahara, T. Yoshioka, M. Asaeda, *J. Colloid Interface Sci.* 228 (2000) 292–296.
- [36] D.R. Machado, D. Hasson, R. Semiat, *J. Membr. Sci.* 163 (1999) 93–102.
- [37] B. Bettens, S. Dekeyser, B. Van, J. der Bruggen, C. Degreve, J. Vandecasteele, *Phys. Chem. B* 109 (2005) 5216–5222.
- [38] T. Mohammadi, A. Aroujalian, A. Bakhshi, *Chem. Eng. Sci.* 60 (2005) 1875–1880.
- [39] J. Li, C. Chan, B. Han, Y. Peng, J. Zou, W. Jiang, *J. Membr. Sci.* 203 (2002) 127–136.
- [40] X. Chen, Z. Ping, Y. Long, *J. Appl. Polym. Sci.* 67 (1998) 629–636.
- [41] P. Sampranpiboon, R. Jiratananon, D. Uttapap, X. Feng, R.Y.M. Huang, *J. Membr. Sci.* 174 (2000) 55–65.
- [42] L.M. Vane, V.N. Nambodiri, T.C. Bowen, *J. Membr. Sci.* 308 (2008) 230–241.
- [43] S.M. Klein, W.H. Abraham, *AIChE Symp. Ser.* 79 (230) (1983) 53.
- [44] L. Liang, E. Ruckenstein, *J. Membr. Sci.* 114 (1996) 227–234.
- [45] D.R. Lide, *CRC Handbook of Chemistry and Physics: A Ready-reference Book of Chemical and Physical Data*, CRC, 2005.
- [46] M.V. Chandak, Y.S. Lin, W. Ji, R.J. Higgins, *J. Membr. Sci.* 133 (1997) 231–243.
- [47] Sowmya Ganapathi-Desai, Subhas K. Sikdar, *Clean Products Processes* 2 (2000) 140–148.